Decoherence, tunneling, and noise-induced activation in a double-potential well at high and zero temperature

Nuno D. Antunes,[1,*] Fernando C. Lombardo,[2,†] Diana Monteoliva,[3,‡] and Paula I. Villar[2,§]
[1]*Centre for Theoretical Physics, University of Sussex, Falmer, Brighton BN1 9QJ, United Kingdom*
[2]*Departamento de Física Juan José Giambiagi, FCEyN UBA, Facultad de Ciencias Exactas y Naturales, Ciudad Universitaria, Pabellón I, 1428 Buenos Aires, Argentina*
[3]*Departamento de Física, Facultad de Ciencias Exactas de la Universidad Nacional de La Plata, La Plata, Argentina*
(Received 1 August 2005; revised manuscript received 3 March 2006; published 2 June 2006)

We study the effects of the environment on tunneling in an open system described by a static double-well potential. We describe the evolution of a quantum state localized in one of the minima of the potential at $t=0$, in both the limits of high and zero environment temperature. We show that the evolution of the system can be summarized in terms of three main physical phenomena—namely, decoherence, quantum tunneling, and noise-induced activation—and we obtain analytical estimates for the corresponding time scales. These analytical predictions are confirmed by large-scale numerical simulations, providing a detailed picture of the main stages of the evolution and of the relevant dynamical processes.

DOI: 10.1103/PhysRevE.73.066105 PACS number(s): 05.60.Gg, 03.65.Yz, 03.70+k, 05.40.Ca

I. INTRODUCTION

The emergence of classical behavior in quantum systems is a topic of great interest from both the conceptual and experimental points of view [1]. It is well established by now that the interaction between a quantum system and an external environment can lead to its classicalization, decoherence and the occurrence of classical correlations being the main features of this process (for a recent overview see [2]).

One of the most intriguing prospects in quantum physics is the possibility of observing quantum tunneling on macroscopic scales [3,4]. Macroscopic systems are generally open systems, interacting with an external environment, and in this context quantum tunneling is qualitative different from its experimentally verified microscopic analog [5].

The analysis of open systems has led to interesting results, detailing the dynamics of a quantum system coupled to a thermal bath with arbitrary temperature. A closed quantum system described by a state localized around a metastable minimum should tunnel through the potential barrier with a well-defined time scale. This tunneling time can be estimated using standard techniques such as the instaton method [6]. For an open system, on the other hand, it is well known that the environment induces decoherence on the quantum particle, its behavior becoming classical as soon as interference terms are destroyed by the external noise [7]. This transition from a quantum to a classical behavior is forced by the interaction with a robust environment and takes place at a given time scale, the decoherence time [8]. This quantity depends on the properties of the system, its environment, and their mutual coupling. If the decoherence time is significantly smaller than the tunneling time, one would expect that after classicalization the state should become confined to the metastable vacuum, with tunneling being suppressed. The particle could still cross the barrier but only if excited by the bath, its energy increasing via thermal activation, for example. This process is distinct from quantum tunneling, is classical in its nature, and should be efficient mostly at high environmental temperatures.

An interesting question arises: what is the effect on tunneling if the particle is coupled to a reservoir at zero temperature? Though in this case there should be in principle no thermal activation, we know there is decoherence induced by a quantum environment at zero temperature [2,9–11]. This would lead to classicalization, and one could conclude that even at $T=0$, quantum tunneling should be inhibited by interaction with the external environment [12].

The study of the effects of an external environment on tunneling was initiated by Caldeira and Legget [3] who showed that dissipation inhibits tunneling. Dissipation in the primary system is not the only result of the interaction with the external environment. Not only does the bath lead to the renormalization of the coupling constants and of the frequency, but its dissipation induces fluctuation (noise) on the system as well [13]. Since this groundbreaking study [3,14], many other works have looked at the various aspects of the same phenomenon, arriving more often than not at similar conclusions [15]. What is even more appealing is the fact that nearly all studies rely on analytical techniques, either functional-based approaches or generalizations of instanton-type calculations. These approaches are based on equilibrium concepts and may miss important dynamical aspects of the evolution. In particular, it is hard to treat both tunneling and activationlike effects simultaneously and to differentiate their individual contributions to the outcomes.

Since the early works on open quantum systems, computational power has increased hugely and it is now feasible to test and extend many analytical results using large-scale numerical simulations. In the context of simulations of open systems with tunneling effects, the main focus has been on driven systems, where tunneling between regular and nonregular islands is of interest [16,17]. In these models, the

*Electronic address: n.d.antunes@sussex.ac.uk
†Electronic address: lombardo@df.uba.ar
‡Electronic address: monteoli@df.uba.ar
§Electronic address: paula@df.uba.ar

interplay of classical chaos and dissipation bears interesting effects at the boundary between classical and quantum mechanics—e.g., the elimination of classical chaos by quantum interference or its restoration by dissipation.

In this article we will concentrate on a simple tunneling system described by a static Hamiltonian. Specifically, we will look in detail at the evolution of a particle in a quantum state localized at one of the minima of a double-well potential, when coupled to an external environment at both zero and high temperature. We will present an analytical description of the effects of dissipation and diffusion and estimate the time scales associated with the distinct physical processes governing the dynamics of the system: decoherence, quantum tunneling, and activation. Using large-scale numerical simulations we will then be able to obtain a full description of the dynamics of the model and test the analytical estimates. Moreover, since we will have access to the state of the system at any time, we will be able to distinguish between the effects of the several processes mentioned above.

As we will discuss below, we confirm that in the high-temperature regime, the evolution can be indeed well understood in terms of simple decoherence, tunneling, and activation time scales. This sheds light on the problem conceptually and offers a great degree of control over the behavior of the system. In particular, we will see how the environment can be manipulated in order to delay or accelerate decoherence and how the strength of the bath's coupling allows activation to be retarded. The estimates provided can be used in wider situations and hopefully be generalized to realistic systems with tunneling on macroscopic scales. Finally, we will show than in the particular case of a zero-temperature environment, not only is tunneling inhibited, but contrarily to what may be naively expected, noise activation is also observed. Consequently, at large times after decoherence, the particle has always a nonzero probability of crossing the potential barrier. We will discuss how this result can be understood by means of a classical finite-temperature analog.

The paper is organized as follows. In Sec. II we present our model and derive estimates of the relevant scales involved. In Sec. III we analyze the high-temperature limit, showing how decoherence inhibits tunneling and describing thermal activation in the classical regime. This is done using both analytical and numerical results. Sec. IV contains a similar analysis detailing the case of zero environmental temperature. Finally, in Sec. V, we include our final remarks and in the Appendix we expand on more technical details of calculations relevant for the body of the paper.

II. THE MODEL

We will start by considering a quantum anharmonic oscillator with a potential given by $V(x)=-\frac{1}{4}\Omega^2x^2+\lambda x^4$. This is a double-well potential with two absolute minima at $x_0=\pm\Omega/\sqrt{8\lambda}$ separated by a potential barrier with height $V_0=\Omega^4/(64\lambda)$. We will assume that the system is open, meaning that it is coupled to an environment composed of an infinite set of harmonic oscillators [18]. The complete classical action for the system and environment is given by

$$S[x,q_n]=S_{\rm sys}[x]+S_{\rm env}[q_n]+S_{\rm int}[x,q_n]$$
$$=\int_0^t ds\left[\frac{1}{2}\dot{x}^2+\frac{1}{4}\Omega^2x^2-\lambda x^4+\sum_n\frac{1}{2}m_n(\dot{q}_n^2-\omega_n^2q_n^2)\right]$$
$$-\sum_n C_nxq_n, \tag{1}$$

where q_n, m_n, and ω_n are, respectively, the coordinates, masses, and frequencies of the environmental oscillators. The mass of the anharmonic oscillator is set to 1. The main system is coupled linearly to each oscillator in the bath with strength C_n. This action describes one of the most simple quantum Brownian motion (QBM) models, which has been widely used in the study of quantum-to-classical transition phenomena [7,13].

The dynamics of the nonlinear oscillator can be obtained by tracing over the degrees of freedom of the environment and obtaining a master equation for the reduced density matrix of the system, $\rho_{\rm r}(t)$. We will assume that the initial states of the system and environment are uncorrelated, with the latter being in thermal equilibrium at temperature T (possibly zero) for $t=0$ (i.e., when the interaction between the system and environment is switched on). At the initial time, the state is a product of a given state of system (entirely on the left well) and a thermal state for the environment. Only when the interaction is turned on is the system allowed to evolve. The initial condition is not an equilibrium state of the complete action. Under these assumptions and using the fact that the system-environment coupling is small, the reduced density matrix satisfies the following time-convolutionless master equation [19]:

$$\dot{\rho}_{\rm r}(t)=-i[H_{\rm sys},\rho_{\rm r}(t)]-\int_0^t d\tau\{\nu(\tau)[x(t),[x(-\tau),\rho_{\rm r}(t)]]$$
$$-\imath\eta(\tau)[x(t),\{x(-\tau),\rho_{\rm r}(t)\}]\}. \tag{2}$$

This equation is perturbative, and therefore we will work with a reduced density matrix which is obtained in second order of the system-environment coupling. This fact will be taken into account in all the simulations we will present. We will work in the underdamped case, which ensures the validity of the perturbative solutions up to the times we are interested in [13,17]. Hereafter, let us have the Ohmic environment in mind and envisage the situation in which $\gamma_0\ll\hbar$, which is called the weak-interaction situation and sets the temporal domain for perturbative solutions. All the results obtained below are for periods of the evolution well within the regime for which this approximation is valid [20]. $H_{\rm sys}$ is the Hamiltonian for the closed system, and $x(t)=e^{iH_{\rm sys}t}xe^{-iH_{\rm sys}t}$ the position operator in the Heisenberg picture. Here and in the following, we will work in units of $\hbar=1$. η and ν are the dissipation and noise kernels, respectively, defined as

$$\eta(t)=\int_0^\infty d\omega I(\omega)\sin\omega t, \tag{3}$$

$$\nu(t) = \int_0^\infty d\omega I(\omega) \coth \frac{\beta\omega}{2} \cos \omega t, \tag{4}$$

where $I(\omega)=\Sigma_n C_n^2 \frac{\delta(\omega-\omega_n)}{2m_n\omega_n}$ is the spectral density of the environment and $\beta=1/T$ its inverse temperature (with the Boltzmann constant set to unity, $k_B=1$). It is worth noting that Eq. (2) is valid at any temperature and is local in time, despite the fact that no Markovian approximation was explicitly taken. In the next few sections, we will show how the general master equation simplifies in different regimes, making it more tractable for both analytical and numerical techniques.

As discussed in Sec. I, we are interested in studying tunnelinglike phenomena. With this in mind, we will look at the evolution of a state for which the particle is initially localized in one of the sides of the double potential well. In particular, we take as initial condition for the main system a Gaussian wave function centered around the left-hand minimum of the potential, $x_0=-\Omega/\sqrt{8\lambda}$:

$$\Psi_0(x) = \frac{1}{(2\pi\sigma_x^2)^{1/4}} \exp\left[-\frac{(x-x_0)^2}{4\sigma_x^2}\right]. \tag{5}$$

The width of the Gaussian is set to $\sigma_x=1/\sqrt{2\Omega}$, corresponding to the vacuum state for a harmonic oscillator with frequency Ω. At this point we should take into account that once the main system is coupled to the environment, the oscillator changes its frequency to a shifted one due to the coupling. We will set parameters in order that this frequency shift can be neglected at all times (we will come back to this point below, when we discuss numerical results at zero temperature). The frequency Ω is the natural frequency obtained by expanding $V(x)$ in the vicinity of its minimum x_0 with $\Psi_0(x)$; thus, it describes a particle which is "locally" in the "vacuum." For the closed system, we expect the state to tunnel through the potential barrier: after a tunneling time τ, the wave function should be approximately given by a Gaussian with similar width centered on the right-hand minimum of the potential. The tunneling time can be estimated using standard techniques. The initial Gaussian is well approximated by a linear combination of the first two energy eigenstates of the full potential $V(x)$. Denoting the energies of the symmetric and antisymmetric eigenstates by E_0 and E_1, respectively, we expect the tunneling time to be given by $\tau \simeq 1/(E_1-E_0)$. However, as the initial condition, Eq. (5), is not an exact sum of the two eigenstates, there will be a correction in the tunneling time. Numerically, as discussed below, we found that in general $\tau=3/(E_1-E_0)$. The energy difference and corresponding tunneling time can be obtained by a straightforward instanton calculation [6], the final result being

$$\tau = \frac{3}{E_1-E_0} = \frac{3}{8}\sqrt{\frac{\pi}{2}\frac{\Omega}{V_0}}\frac{1}{\Omega}\exp\left[\frac{16}{3}\frac{V_0}{\Omega}\right]. \tag{6}$$

The expression inside the exponential is the classical action for the instanton, $S_0=(16/3)V_0/\Omega$.

III. TUNNELING INHIBITION AT HIGH T

At high temperature the reduced master equation can be expressed in a much simplified way by means of the (also reduced) Wigner distribution function on phase space, $W=W(x,p;t)$ [2,7]:

$$\dot{W} = \{H_{\rm sys}, W\}_{\rm PB} - \frac{\lambda}{4} x\partial_{ppp}^3 W + 2\gamma(t)\partial_p(pW) + D(t)\partial_{pp}^2 W - f(t)\partial_{px}^2 W, \tag{7}$$

where

$$\gamma(t) = -\frac{1}{2\Omega}\int_0^t d\tau \sin(\Omega\tau)\eta(\tau), \tag{8}$$

$$D(t) = \int_0^t d\tau \cos(\Omega\tau)\nu(\tau), \tag{9}$$

$$f(t) = -\frac{1}{\Omega}\int_0^t d\tau \sin(\Omega\tau)\eta(\tau). \tag{10}$$

$\gamma(t)$ is the dissipation coefficient, and $D(t)$ and $f(t)$ are the diffusion coefficients, all of them given in terms of the dissipation and noise kernels defined in Eqs. (3) and (4). The first term on the right-hand side of Eq. (7) is the Poisson brackets, corresponding to the usual classical evolution. The second term includes the quantum corrections to the dynamics. The last three terms describe dissipation and diffusion effects due to the coupling to the environment. In order to simplify the problem, we consider a high-temperature Ohmic environment; i.e., we take $I(\omega)=\frac{2}{\pi}\gamma_0\omega\frac{\Lambda^2}{\Lambda^2+\omega^2}$, where Λ is a high-frequency cutoff which is larger than any frequency involved in the system. In this approximation the coefficients in Eq. (7) become constant in time: $\gamma=\gamma_0$, $f\sim 1/T$, and $D=2\gamma_0 T$. The anomalous diffusion coefficient f is much smaller than the other ones, and therefore we neglect it in Eq. (7). It is important to note that the high-temperature approximation is well defined only after a time scale of the order of $1/T\sim\gamma_0/D$. For all cases we will be studying the relevant period of the evolution lies at much later times, well in the regime where the approximation holds on.

As discussed in Sec. I, the thermal bath will have two distinct effects on the evolution of the initial wave packet. In a regime where the weak coupling to the environment is strong enough, the diffusion will make the initial quantum packet decohere, quantum interference terms will be suppressed, and the system will behave classically. After the decoherence time $t_{\rm D}$, quantum behavior will be inhibited and tunneling should not be possible any longer. Because the initial energy of the particle is less than the barrier height V_0, we would expect it to remain localized on the initial side of the barrier after $t_{\rm D}$. On the other hand, since the particle is in contact with a high-temperature environment, it will "warm up" and in time its energy will increase. At some time $t_{\rm th}$ there will be a significant probability for the particle to cross through the top of the barrier, via thermal activation. For

very long times, the system should reach a state of thermal equilibrium, with the particle being equally likely to be found on either side of the barrier.

We will now estimate these two time scales. In particular, we will be interested in understanding how t_D and t_{th} interplay with each other, making the crossing of the barrier more or less likely at different stages of the evolution.

The decoherence time in the high-T limit is usually assumed to be inversely proportional to the diffusion term D and to the square of the spatial extension of the wave packet L. For our choice of initial conditions we assume that for early times L can be set to the width of the original Gaussian wave function—that is, $L=2\sigma_x=2/\sqrt{2\Omega}$. Using $D=2\gamma_0 T$ we obtain (in units of $\hbar=1$) [7]

$$t_D = \frac{\Omega}{4\gamma_0 T}. \tag{11}$$

Though the result is not exact, with t_D being slightly overestimated due to the choice of L, its accuracy is enough for our purposes.

The thermal activation rate for a classical system can be obtained by working with the classical analog of Eq. (7), the Fokker-Planck equation:

$$\dot{W} = \{H_{sys}, W\}_{PB} + 2\gamma_0 \partial_p (pW) + D\partial_{pp}^2 W. \tag{12}$$

Note that after decoherence takes place and quantum terms become irrelevant for the evolution, Eq. (7) reduces to Eq. (12). The classical evolution for the average of any physical observable $A(x,p)$ in this regime is then given by

$$\partial_t \langle A\rangle = -\langle \{H_{sys}, A\}_{PB}\rangle + D\langle \partial_p^2 A\rangle - 2\gamma_0 \langle p\partial_p A\rangle. \tag{13}$$

If we take $A(x,p)$ to be the Hamiltonian of the main system, we obtain $\partial_t\langle H\rangle = 2\gamma_0(T-\langle p^2\rangle)$. This expression can be further simplified by assuming T to be much higher than the relevant energy scales in the problem, V_0 and $\langle p^2\rangle$, during the early stages of the evolution. As a result, the time dependence of the energy of the system is given by

$$\partial_t\langle H\rangle = 2\gamma_0 T \rightarrow E = E_0 + 2\gamma_0 T t, \tag{14}$$

where E_0 is the initial energy of the system. We can then estimate the thermal activation time t_{th} to be of the same order of the time it takes the system to reach, on average, the energy of the height of the barrier:

$$t_{th} = \frac{V_0 - E_0}{2\gamma_0 T}. \tag{15}$$

When the energy of the initial state is considerably smaller than the potential height this reduces to $t_{th}=V_0/(2\gamma_0 T)$. These estimates clearly show that there is a large region of parameter space where it is possible to have decoherence taking place before the tunneling time and delay considerably thermal activation. In these cases the particle should remain confined in the original side of the barrier as long as $t<t_{th}$. Ideally we would like to have t_D and t_{th} separated as much as possible from the tunneling time scale τ—that is, $t_D \ll \tau \ll t_{th}$. For practical purposes we write

$$a t_D = \tau = b t_{th}. \tag{16}$$

From the first and last terms we find a restriction on the parameters of the potential:

$$\frac{V_0}{\Omega} = \frac{1}{2}\left(\frac{a}{b} + 1\right). \tag{17}$$

Together with a choice of tunneling time, Eq. (17) fixes the potential of the main system. The parameters of the environment can then be set using the first part of Eq. (16):

$$\gamma_0 T = \frac{a\Omega}{4\tau}. \tag{18}$$

A choice of $a \gg 1$ and $b \ll 1$ would lead to the desired result, keeping the particle localized one side of the potential well for an arbitrary long time.

A. Numerical simulation

Our goal here is to use a numerical simulation to test and illustrate the suppression mechanism discussed above. In terms of the notation of Eq. (16) we should favor a system with large a and small b. Though such values are perfectly admissible physically, they correspond to a situation which is hard to tackle numerically. From Eq. (17) we see that a large ratio of a to b implies a high value for V_0/Ω. This quantity $n=V_0/\Omega$ is none other than the semiclassical estimate for the number of states trapped in the potential well. As we will discuss below, our numerical method is based on evolving an equation for the eigenstates, which will be in large number. Since the tunneling time depends exponentially on n, we will also be faced with very large integration times. As a consequence we will have to choose "conservative" values for a and b. Nevertheless, the results will still describe in a conclusive way the phenomena described in the previous section.

1. Numerical method

The master equation (7) can only be solved by step-by-step methods up to relatively short times. As a way out of this problem we resorted to numerically integrating Eq. (2) on the basis $|\mu\rangle$ of eigenstates of the Hamiltonian of the isolated system, $H_{sys}=\frac{p^2}{2}+V(x)$. In our high-$T$ limit this reduces to

$$\dot{\rho}_{\mu\nu} = -\sum_{\alpha\beta} M_{\mu\nu\alpha\beta}\rho_{\alpha\beta}, \tag{19}$$

where M is *time independent*. The full expression for M can be found in the Appendix. We have for notation simplicity dropped the subindex "r" on ρ_r.

As Eq. (19) has *constant* coefficients, it can be integrated up to *any* time once the coefficients M are numerically calculated. That means that we can write the exact solution of the master equation (19) in terms of M as

$$\rho_{\mu\nu} = \sum_{\alpha\beta} (e^{-Mt})_{\mu\nu\alpha\beta}\rho_{\alpha\beta}(0). \tag{20}$$

All the difficulty is now shifted to the calculation of the eigenstates $|\mu\rangle$ of the system H_{sys}, the construction of M, and

the calculation of its exponential. Here problems may arise since M has dimension N^4 (where N is the dimension of the space representing the real Hilbert space of the problem). Thus N should not be too large. On the other hand, the number N of states should be large enough to faithfully represent the system's Hilbert space: as decoherence couples these states, the expected quasiequilibrium state resulting from the master equation should be diagonal in the eigenstate basis. The master equation tends to mix these states in such a way that the entropy grows to a level where all states become occupied with equal probability. This provides a good criterion for the validity of the numerical simulation—in practice, we will trust the numerical solution of the master equation only up to times when the entropy S is below saturation—i.e., $S < S_{\mathrm{sat}} = \ln N$.

2. Decoherence inhibits tunneling

We have solved Eq. (19) for the system parameters $V_0 = 100$ and $\Omega = 5$, which leads to $n = 20$. For this set of parameters the estimated tunneling time is $\tau = 4.631\,554\,03 \times 10^{10}$. We have chosen $a = 24.5$ and $b = 0.6282$ so that $\gamma_0 T = 3.9 \times 10^{-11}$, which is a very small value. This is to be desired so that the system heats very slowly, delaying thermal activation until after the tunneling time. Finally, we obtain the relation between the three time scales $t_D \sim 0.0408\tau$ and $t_{\mathrm{th}} \sim 1.6326\tau$.

As the initial state is well expanded by ten eigenstates of H_{sys} and $n = 20$, we have chosen a Hilbert space with $N = 40$ which is as large a value of N as we can afford numerically. The environment high-frequency cutoff is set to $\Lambda = 10\Delta_{40,0} = 10 \times 102.237\,307 \gg \Delta_{\alpha\beta}$ for all α, β. $\Delta_{\alpha\beta}$ is the frequency separation for eigenstates α and β.

For the numerical solution of the isolated system we have very accurately calculated the eigenstates and eigenvalues of the H_{sys} checking that the tunneling time of our initial state (5) is indeed very close to that estimated by Eq. (6). This is illustrated in Fig. 1 where we show the time evolution of the probability of finding the particle in the original well, for both the isolated and open systems. Starting from unity at $t = 0$, the probability for the former decreases as the particle tunnels through the barrier, reaching zero when $t \simeq \tau$. For longer times (not shown in the figure) the particle tunnels back and forth between the two wells, and as expected, the probability is seen to oscillate with a period close to 2τ. The behavior of the open system is in marked contrast with this. The probability of remaining in the original well decreases but at a much slower rate when compared to the open system. As we will see, this decrease is a consequence of thermal activation rather than tunneling, which is suppressed at very early times. The value of the probability never goes to zero; neither are any oscillations observed. In fact, the probability decreases monotonically and for very long times we should expect it to approach 0.5; when the system thermalizes, it is equally probable to find the particle on each side of the barrier. In the same figure we also show the evolution of the linear entropy S_L of the open system in terms of the maximum of entropy allowed for the finite space representing the Hilbert space of the system, $\ln N$, $S_L/\ln N = -\ln[\mathrm{Tr}\rho^2]/\ln N$. After some time the linear entropy reaches saturation, suggesting that the dimension of the finite space ($N = 40$) is too small. As a consequence the numerical results are less reliable after $t \sim \tau$. Nevertheless, it is clear from the plots that decoherence inhibits tunneling well *before* this time.

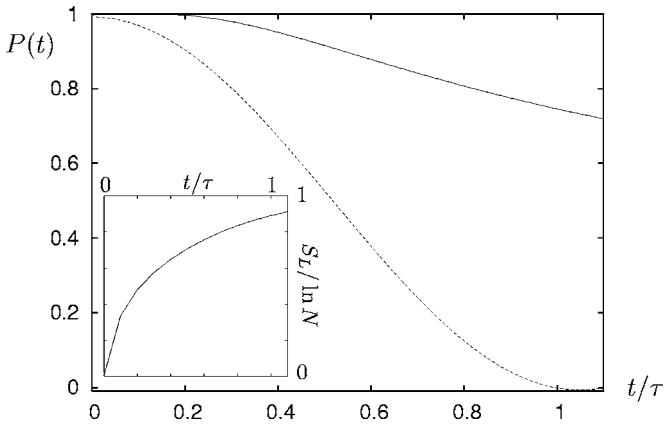

FIG. 1. Time behavior of the probability to stay on the left of the barrier for the open (solid line) and isolated system (dotted line). Time is measured in units of the estimated tunneling time τ. The inset shows, for the same time span, the evolution of the linear entropy of the open system, $S_L/\ln N$, where $N = 40$ is the size of the finite space representing the Hilbert space of the problem. For $t \sim \tau$ the entropy is near saturation, $S_L/\ln N = 1$ (see text).

The qualitative features of the evolution of both the isolated and the open systems are illustrated in Figs. 2 and 3 where we can see, respectively, the probability distribution $\sigma(x,x) = \langle x|\rho_{\mathrm{r}}|x\rangle$ and the Wigner function $W(x,p)$ for significant times. Again, the contrast between their behavior is very clear. For very early times ($t \simeq 0.2\tau$), tunneling starts taking place in the isolated system with $\sigma(x,x)$ becoming nonzero on the right-hand well of the potential. The same effect can be observed in the Wigner function, which also shows nega-

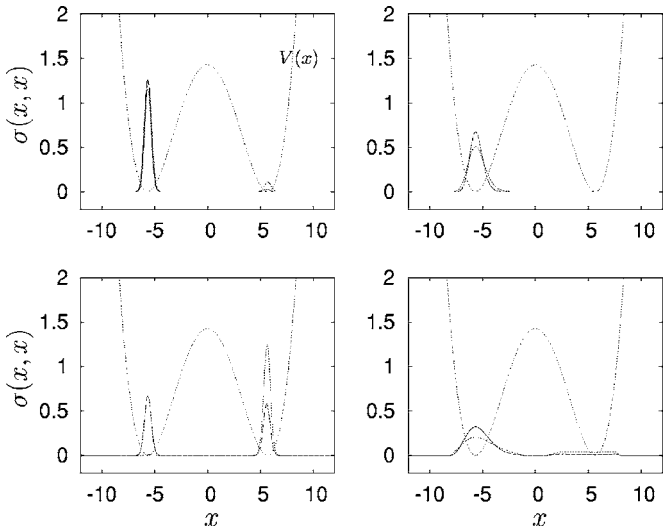

FIG. 2. Probability distribution $\sigma(x,x)$ for the isolated (left) and the open (right) systems for $t = 0$, $t = 0.1\tau$, and $t = 0.2\tau$ (top) and $t = 0$, $t = 0.5\tau$, and $t = \tau$ (bottom). As a reference, the shifted and scaled potential $V(x)$ is drawn in all plots.

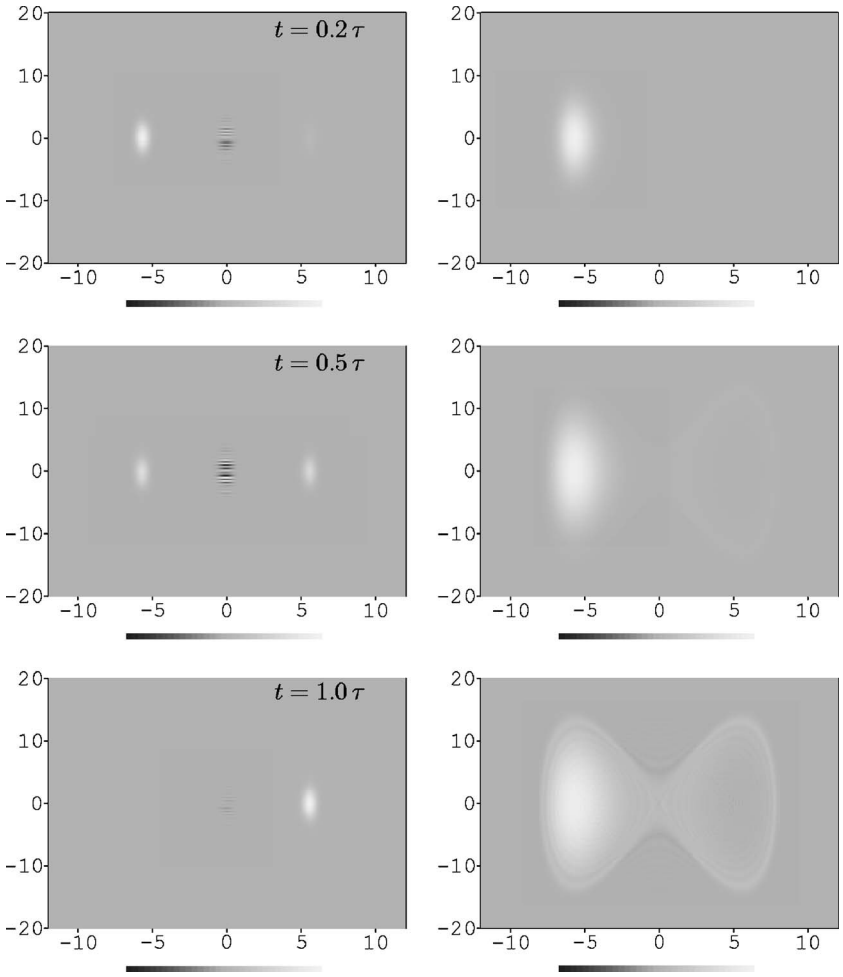

FIG. 3. Wigner distribution functions for the isolated (left) and open (right) systems, for the indicated times. The horizontal axis corresponds to x, vertical axis to p. The medium grey shade on the background corresponds to zero values for the Wigner function, lighter and darker shades, respectively, to positive and negative values of $W(x,p)$.

tive values in the center of the phase space, indicating clear quantum behavior. For the same times, the open system shows no signs of tunneling, with the particle strictly confined to the original side of the potential. The spread of both $\sigma(x,x)$ and $W(x,p)$ increases, as a consequence of diffusion induced by the environment. As expected, since t_D is very small for this system, decoherence has clearly taken place by this time and the Wigner function is strictly positive everywhere. For $t=0.5\tau$, both the probability distribution and the Wigner function are symmetric for the isolated system. On the other hand, the wave packet in the open system has continued to widen and we see the first signs of crossover above the barrier. As the tunneling time is reached, though the system is still mainly localized on the original well, it has become warmer and the Wigner function explores a large region of phase space, with thermal activation becoming significant. Note that since areas of stronger nonlinearity of the potential are now occupied, one can observe slight negative valued fringes in the Wigner function. This transitory behavior is a well-known consequence of the introduction of nonlinear effects in the system and bares no relation with tunneling [21]. At this time, on the other hand, the isolated system has fully tunneled and the wave packet is centered around the right-hand minimum of the potential.

B. Thermal activation in the classical limit

In this section we will present a numerical example of classical high-T thermal activation. Our main goal is to confirm that after decoherence takes place, a quantum system, such as the one studied in Sec. III A, follows the behavior of a purely classical system, displaying thermal activation.

A classical statistical system is described by the Fokker-Planck equation (12). Here, instead of solving Eq. (12) directly to obtain $W(x,p)$, we chose to evolve a very large ensemble of classical particle trajectories interacting with a thermal bath via dissipation and noise terms. The equation of motion for each particle is given by

$$\ddot{x}(t) = -2\gamma_0\dot{x}(t) - V'(x(t)) + \xi(t), \tag{21}$$

where ξ is time-uncorrelated Gaussian noise with variance $\langle\xi(t)\xi(t')\rangle = \gamma_0 T\delta(t-t')$. It is straightforward to show that an ensemble of particles, evolving according to the Langevin equation above, does indeed obey the master equation (12). The numerical solution of a large number of equations of the type of Eq. (21) is trivial, offering an alternative to the direct solution of the master equation as we have done so far. The initial conditions are generated such that x and p are Gaussian random variables distributed according to the classical analog of the wave function, Eq. (5):

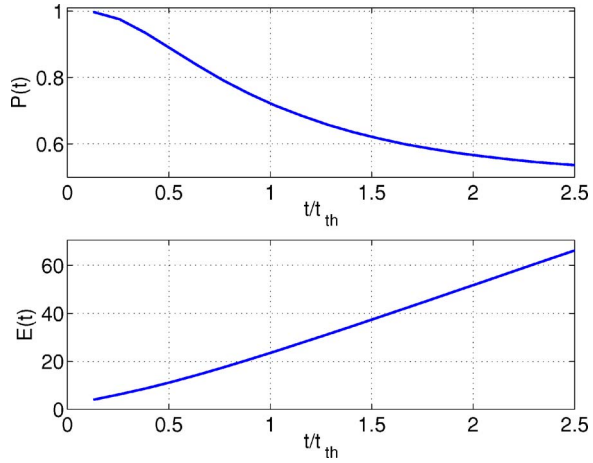

FIG. 4. (Color online) Time dependence of the probability of remaining in the original side of the potential (top) and average energy (bottom). Time is expressed in units of the thermal-activation time scale, Eq. (15).

$$W_0(x,p) = \frac{1}{\pi} \exp\left[-\frac{(x-x_0)^2}{2\sigma_x^2} - 2\sigma_x^2 p^2 \right]. \qquad (22)$$

At arbitrary time t we can obtain expectation values of physical properties by averaging over the ensemble. The Wigner function $W(x,p,t)$ can be determined by evaluating the fraction of particles in the ensemble with position and momentum in the interval $(x,x+dx)(p,p+dp)$.

In Figs. 4 and 5 we show the results of a simulation with $\Omega^2=12$, $V_0=23$, $T=10^7$, and $\gamma_0=2.5\times10^{-9}$. Note that choosing the set of parameters used in Sec. III A would lead to impractical simulation times. The qualitative aspects of the dynamics of the two systems should be similar, though, with the classical simulation illustrating the generic properties of the thermal-activation process.

The thermal-activation time as estimated by Eq. (15) is given, for this set of parameters, by $t_{\rm th}=390$. In Fig. 4 we show both the probability of finding the particle on the left-hand side of the potential and the mean energy of the system. As expected, when $t \simeq t_{\rm th}$ the energy is of the order of the height of the potential barrier. The probability at that time is $P \sim 0.7$. We simulated a series of similar processes with a wide range of parameters and found that Eq. (15) holds very well over several orders of magnitude of the quantities involved. In particular, we found that the "noncrossing" probability at $t=t_{\rm th}$ is always in the range $P \simeq 0.65-0.75$. The probability observed in the quantum simulation of Sec. III A for $t_{\rm th}$ is within this range. This result should be taken qualitatively, though, since $t_{\rm th}$ is reached after entropy saturation has taken place. The overall evolution of $P(t)$ in the classical case follows very closely that for the quantum system after $t_{\rm D}$, with the probability decreasing monotonically and approaching 0.5 for large values of t.

In Fig. 5 we have the phase-space probability distributions (the classical Wigner function) for significant evolution times. Throughout the evolution $W(x,p)>0$, as expected, since the Fokker-Planck equation conserves the positivity of the distribution. As time progresses the initial Gaussian packet widens, its energy increasing and allowing a larger fraction of the ensemble's particles to explore further regions of phase. For $t=t_{\rm th}$, when, as defined, the average particle energy equals the potential height, thermal crossing of the barrier starts to be significant. It is interesting to note that for this period of evolution, the separatrix of the phase space shows a high particle density on the right side of the potential. This confirms that the particles crossing the barrier do so because their energy is of the order of the barrier (corresponding to the separatrix energy). This obvious signature of classical thermal activation can also be observed in the quantum open system in Fig. 3. In the quantum isolated system, on the other hand, the Wigner function remains zero in the separatrix region throughout the evolution. In this case, tunneling can be recognized by the large negative interference

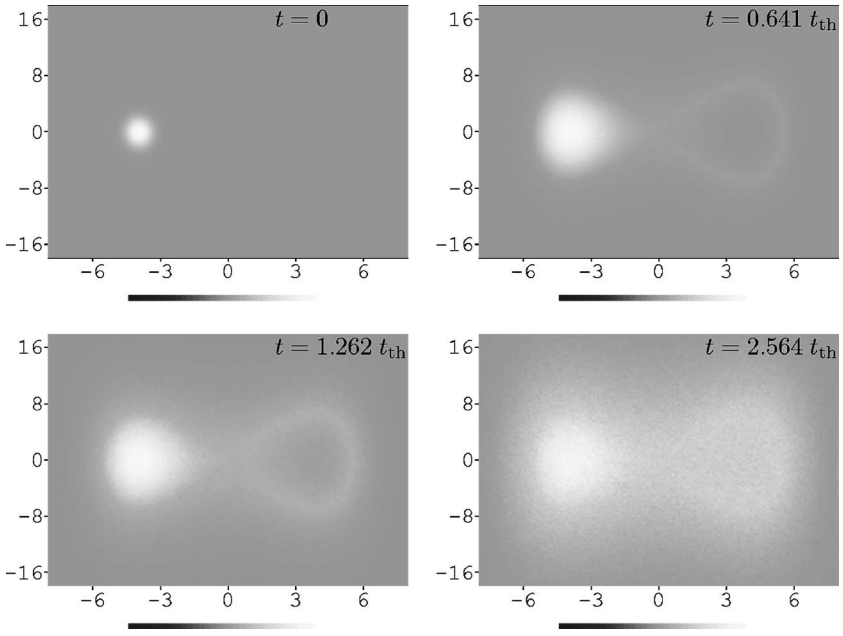

FIG. 5. Classical distribution function of the system for the indicated times. The horizontal axis corresponds to x, vertical axis to p. The medium grey shade on the background corresponds to zero values for the Wigner function, lighter and darker shades, respectively, to positive and negative values of $W(x,p)$

fringes in the origin of the phase space. Back in the classical system, we observe that for large t dissipation and diffusion effects combine to populate the central regions of the right-hand minimum of the potential. Finally, the overall shape of the Wigner function becomes increasingly symmetrical, with the system converging asymptotically to a thermal equilibrium state.

IV. DECOHERENCE AND TUNNELING AT ZERO TEMPERATURE

At $T=0$ the time integrals in the master equation (2) can be explicitly calculated [10]. We focus, as before, on Ohmic environments with spectral density $I(\omega)=\frac{2}{\pi}\gamma_0\omega\frac{\Lambda^2}{\Lambda^2+\omega^2}$. After a rather lengthy calculation, the master equation at $T=0$ on the basis of eigenstates of the isolated system can be written as

$$\dot{\rho}_{\mu\nu} = -i\Delta_{\mu\nu}\rho_{\mu\nu} - \sum_{\alpha\beta}\{D_{\alpha\beta}x_{\mu\alpha}x_{\alpha\beta}\rho_{\beta\nu} - D_{\beta\nu}x_{\mu\alpha}x_{\beta\nu}\rho_{\alpha\beta} - D_{\mu\alpha}x_{\mu\alpha}x_{\beta\nu}\rho_{\alpha\beta} + D_{\alpha\beta}x_{\alpha\beta}x_{\beta\nu}\rho_{\mu\alpha}\} + i\sum_{\alpha\beta}\{\gamma_{\alpha\beta}x_{\mu\alpha}x_{\alpha\beta}\rho_{\beta\nu} + \gamma_{\beta\nu}x_{\mu\alpha}x_{\beta\nu}\rho_{\alpha\beta} - \gamma_{\mu\alpha}x_{\mu\alpha}x_{\beta\nu}\rho_{\alpha\beta} - \gamma_{\alpha\beta}x_{\alpha\beta}x_{\beta\nu}\rho_{\mu\alpha}\}, \quad (23)$$

where the time-dependent complex coefficients $D_{\alpha\beta}=D_{\alpha\beta}(t)$ and $\gamma_{\alpha\beta}=\gamma_{\alpha\beta}(t)$ are given by

$$D_{\alpha\beta} = D(\Delta_{\alpha\beta}) + i\Delta_{\alpha\beta}f(\Delta_{\alpha\beta}), \quad (24)$$

$$\gamma_{\alpha\beta} = -\frac{1}{2}\tilde{\Omega}^2(\Delta_{\alpha\beta}) - i\Delta_{\alpha\beta}\gamma(\Delta_{\alpha\beta}), \quad (25)$$

with

$$D(\Delta) = \frac{2\gamma_0}{\pi}\frac{\Lambda^2\Delta}{\Delta^2+\Lambda^2}\left[\mathrm{Shi}(\Lambda t)\left(\frac{\Lambda}{\Delta}\cos\Delta t\cosh\Lambda t + \sin\Delta t\sinh\Lambda t\right) - \mathrm{Chi}(\Lambda t)\left(\frac{\Lambda}{\Delta}\cos\Delta t\sinh\Lambda t + \sin\Delta t\cosh\Lambda t\right) + \mathrm{Si}(\Delta t)\right],$$

$$f(\Delta) = 2\gamma_0\frac{\Lambda^2}{\Delta^2+\Lambda^2}\left[\mathrm{Shi}(\Lambda t)\left(\frac{\Lambda}{\Delta}\sin\Delta t\cosh\Lambda t - \cos\Delta t\sinh\Lambda t\right) + \mathrm{Chi}(\Lambda t)\left(-\frac{\Lambda}{\Delta}\sin\Delta t\sinh\Lambda t + \cos\Delta t\cosh\Lambda t\right) - \mathrm{Ci}(\Delta t) - \ln\frac{\Lambda}{\Delta}\right] \quad (26)$$

and

$$\tilde{\Omega}^2(\Delta) = -\frac{2\gamma_0\Lambda^3}{\Lambda^2+\Delta^2}\left[1 - e^{-\Lambda t}\left(\cos\Delta t - \frac{\Delta}{\Lambda}\sin\Delta t\right)\right],$$

$$\gamma(\Delta) = \frac{\gamma_0\Lambda^2}{\Lambda^2+\Delta^2}\left[1 - e^{-\Lambda t}\left(\cos\Delta t + \frac{\Lambda}{\Delta}\sin\Delta t\right)\right]. \quad (27)$$

As before, $\Delta_{\alpha\beta}=\omega_\alpha-\omega_\beta$, the frequency difference between eigenstates α and β. The set of coefficients $D_{\alpha\beta}$ encapsulates the effects of diffusion at $T=0$, with $D(\Delta)$ representing the normal diffusion and $f(\Delta)$ the anomalous one. The others represent the effect of the environment through the dissipation kernel η, with $\tilde{\Omega}(\Delta)$ the frequency shift and $\gamma(\Delta)$ the dissipation coefficient. The last two reach constant asymptotic values for $\Lambda t \gg 1$.

Even though the time-dependent functions (26) reach an asymptotic constant value for $\Delta_{\alpha\beta}t \gg 1$ and $\Lambda t \gg 1$, for the problem we are going to analyze we will never reach a regime where all the coefficients involved by Eq. (23) are constant. That is, the expressions in Eqs. (26) are constant for *all* α,β when $t \gg 1/\Lambda$ and $t \gg 1/\Delta_{1,0} \approx \tau/3$, due to Eq. (6). As the functions $\mathrm{Si}(t)$ and $\mathrm{Ci}(t)$ converge toward its asymptotic values only very slowly, we will never reach this regime.

As for the high-T limit we want to estimate the decoherence time scale. For this purpose we will analyze the decoherence process in a simple case: $\Psi(x,t=0)=\Psi_1(x)+\Psi_2(x)$, where

$$\Psi_{1,2} = N\exp\left(-\frac{(x\mp L_0)^2}{2\delta^2}\right)\exp(\pm iP_0x), \quad (28)$$

with N a normalization constant and δ the initial width of the wave packet.

As was defined in the previous literature (see, for example, [2,7]), the effect of decoherence is produced by an exponential factor $\exp(-A_{\mathrm{int}})$, defined as

$$\exp(-A_{\mathrm{int}}) = \frac{1}{2}\frac{W_{\mathrm{int}}(x,p)|_{\mathrm{peak}}}{[\,W_1(x,p)|_{\mathrm{peak}}\,W_2(x,p)|_{\mathrm{peak}}]^{1/2}}, \quad (29)$$

where W_{int} is Wigner's interference term, coming from the superposition of the two states $\Psi_{1,2}$.

In a very crude approximation one may drop all nonlinear terms on the Hamiltonian of the system and then estimate the decoherence time scale from (see Ref. [10] for details)

$$\dot{A}_{\mathrm{int}} \approx 4L_0^2D(\Delta) - 2f(\Delta), \quad (30)$$

where L_0 is the spread of the state. In order to evaluate the decoherence time t_{D}, we have to solve $1 \approx A_{\mathrm{int}}(t=t_{\mathrm{D}})$. From Eq. (30) it is not possible to find a global decoherence time scale at $T=0$. Nevertheless, we can find limits in which we are able to give different scales for decoherence.

When $\Delta t \ll 1$ (for times $\frac{1}{\Lambda} < t < \frac{1}{\Delta}$), we can approximate A_{int} using the asymptotic limits of Si and Ci by

$$A_{\mathrm{int}} \approx \frac{8\Lambda^2}{\Lambda^2+\Delta^2}\gamma_0\left[\frac{L_0^2}{2\pi}(\Delta t)^2 + t(\ln\Lambda t + \Gamma - 1)\right], \quad (31)$$

resulting in a decoherence time bound

$$t_D \leqslant \frac{1}{8\gamma_0}. \quad (32)$$

For large frequency Δ, such as $\Delta \sim \Lambda$, it is easy to see that

$$A_{\mathrm{int}} \sim 2L_0^2\gamma_0\Lambda t + 4\gamma_0\left(t\,\mathrm{Ci}(\Lambda t) - \frac{\sin\Lambda t}{\Lambda}\right), \quad (33)$$

giving a very short decoherence time scale

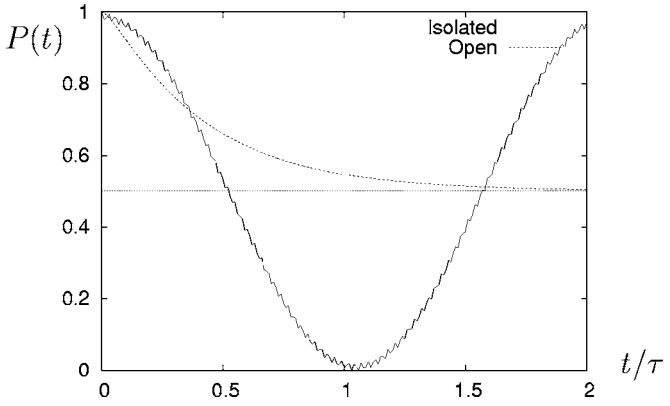

FIG. 6. Time behavior of the probability to stay on the left of the barrier. Time is measured in units of the estimated tunneling time τ.

$$t_D \sim \frac{1}{2L_0^2\gamma_0\Lambda}. \tag{34}$$

This result will be valid as long as the product $L_0^2\gamma_0 \leqslant 1$, allowing us to neglect the initial transient.

As this decoherence time scale was derived after dropping all nonlinear terms on the Hamiltonian of the system, it is then valid only for linear systems. We can only expect it to be of some use when we begin with a narrow initial state located at one of the potential minima of the system because for a while it will evolve as in an harmonic oscillator potential. After some (short) time the nonlinearities will generate interferences dynamically [21]. Then, we should expect Eq. (32) to be only accurate if decoherence happens early enough, before nonlinear effects kick in.

Numerical results

We have numerically solved Eq. (23) using a standard adaptative-step-size fifth-order Runge-Kutta method for different parameters of the system and the environment. All results were found to be robust under changes in the parameters of the integration method.

As an example we have chosen $\Omega=100$ and $V_0=200$ for the system for which the estimated tunneling time scale is $\tau \approx 158.27$. As for the high-T limit, we desire decoherence to occur before tunneling, so we have set the parameters of the environment according to $at_D=\tau$ with $a=10$. Then from Eq. (32) $\gamma_0=a/(8\tau)\approx 0.007\,897$. We set the frequency cutoff to $\Lambda=10V_0=2000$. With this set of parameters and taking into account Eq. (27), we see that the effects of the frequency shift in the initial state can be neglected. In fact, it is easy to check that for these values, $\tilde{\Omega}^2$ is 0.32% of Ω^2. Therefore we can safely neglect the error induced by taking the initial state to be given by the vacuum of an harmonic oscillator of frequency Ω, rather than $\tilde{\Omega}$.

Figure 6 shows the probability of staying in the original well, $P(t)=\int_{-\infty}^{0} dx\sigma(x,x)$, in terms of the time measured in units of the estimated tunneling time τ, while Figs. 7 and 8 show the probability distribution $\sigma(x,x)$ and the Wigner function of the system, respectively, for the indicated times, for both the isolated and open systems.

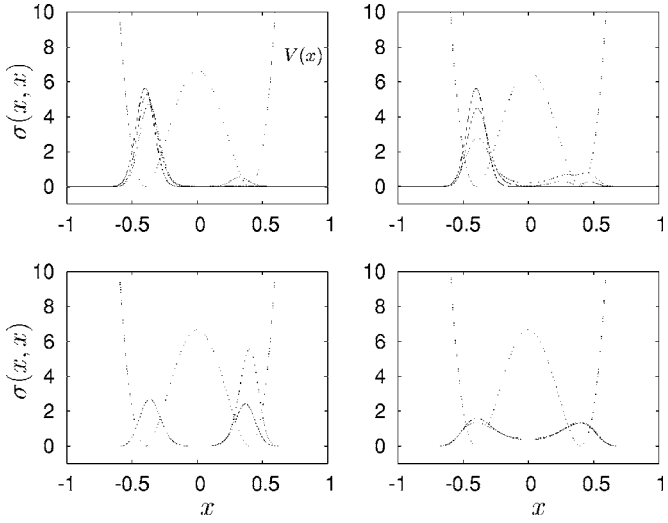

FIG. 7. Probability distribution $\sigma(x,x)$ for the isolated (left) and open (right) systems for $t=0$, $t=0.1\tau$, and $t=0.2\tau$ (top) and $t=0.5\tau$ and $t=\tau$ (bottom). As a helpful reference, the scaled potential $V(x)$ is drawn in all the plots.

The evolution of the open system at zero temperature shows similarities but also relevant differences with the analogous situation in the high-T limit. For very early times the probability of staying on the initial side of the potential decreases quickly, approaching 0.5 as soon as $t\sim 2\tau$. There are no signs of the particle tunneling back, as expected, since t_D is taken to be smaller than the tunneling time scale. Also, the asymptotic behavior of $P(t)$ shows no oscillatory behavior as would be expected if tunneling played any role in the late-time dynamics. Instead we see what looks like a quick "equilibration" into a state where the particle is equally likely to be on either side of the potential barrier. Both the probability distribution plots and the Wigner functions corroborate this picture. From very early times, the negative regions of $W(x,p)$ in the $T=0$ case are considerably suppressed when compared with the closed system, suggesting that tunneling has a small contribution to the evolution. For $t>\tau/2$, $W(x,p)$ becomes positive definite and the system displays no tunneling oscillations. As in the high-T case, the separatrix becomes densely populated when cross over starts being significant. Both this and the fact that for late times $\sigma(x,x)$ and $W(x,p)$ are symmetrical around $x=0$ suggests we should be able to describe the dynamics of the open system in terms akin to classical activation.

When trying to interpret the post-decoherence behavior of the open system, several features of its dynamics should be kept in mind. First, one should emphasize that the initial condition is clearly not the ground state of the total action, Eq. (1). As soon as the interaction between the main system and the environment is turned on, at $t=0$, the system will find itself in an excited state. In relation to the new minima of the potential, the environment will have a nonzero amount of energy. From a purely classical point of view, this energy cannot be responsible for the excitation of the particle over the potential barrier. In fact, the height of the potential increases in relation to the new vacuum, in a way such that the *total* energy of the full system is still lower than the barrier

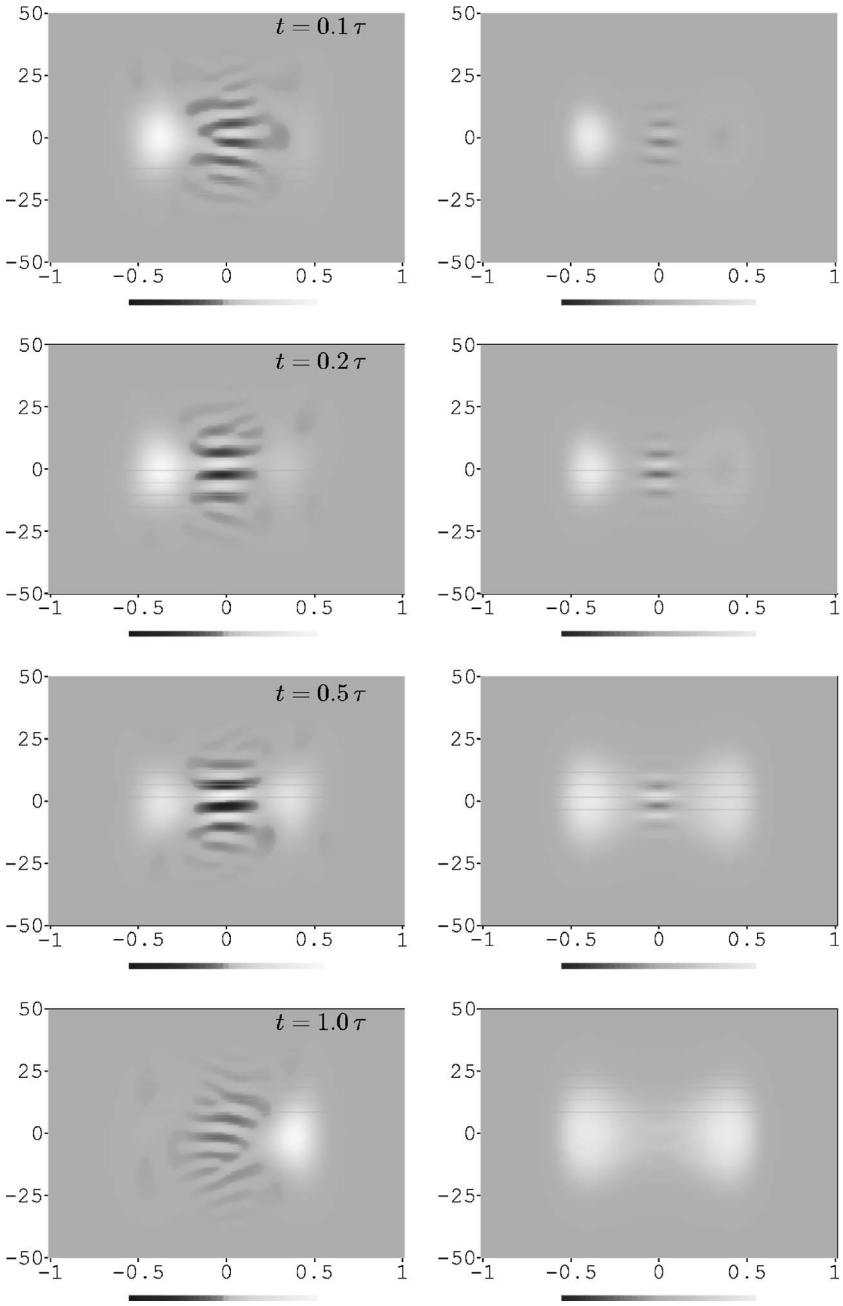

FIG. 8. Wigner distribution functions for the isolated (left) and open (right) systems, for the indicated times. Axes and gray shades are similar to the ones defined in Fig. 3.

separating regions of positive and negative x. This argument can be made more quantitative in the following way: the full potential for the system plus environment is $V(x,q_n) = V_{\text{sys}}(x) + V_{\text{env}}(q_n) + V_{\text{int}}(x,q_n)$ with $V_{\text{sys}}(x) = -1/4\Omega^2 x^2 + \lambda x^4$, $V_{\text{env}}(q_n) = \Sigma_n 1/2\omega^2 m_n^2 q_n^2$, and $V_{\text{int}}(x,q_n) = \Sigma_n C_n x q_n$. Classically, the initial condition is $x = -\Omega/\sqrt{(8\lambda)}$, and because the environment is at $T=0$, $q_n=0$. So, for the full action, the energy terms of the initial condition are given by $V_{\text{sys}} = -\Omega^4/(64\lambda) = V_0$ (the minimum of V_{sys}), $V_{\text{env}}=0$, and $V_{\text{int}}=0$, and so $V=V_0$. Note that, classically, the value of the total energy is the same as the energy of the isolated main particle, even when the interaction with the environment is "switched on." This is a consequence of taking zero temperature for the environment. It is true that when the full system is considered, we are no longer in the state of the minimum of energy, V_0, corresponding to an excited state. Nevertheless, this initial energy cannot be responsible for making the particle cross the potential barrier. The classical trajectory of a particle going over the barrier would have necessarily $x=0$ at some point. If $x=0$, the value for the total energy must be positive $V>0$. Since for the initial state implies $V_0<0$, this can never happen. In other words, when the interaction is switched on, the system does "gain" energy relatively to the new vacuum, but the height of the barrier increases by the same amount, so classical activation cannot take place.

Note that the fact that there are no fluctuations in the environment classically at $T=0$ plays a crucial role in this reasoning. Even for small but finite T, the energy of the environment would go as T. By choosing T small enough, this contribution could always be made smaller than the barrier height. As a consequence and in contrast with the high-T

case, we will not be able to describe the evolution of the quantum system after classicalization by simply taking its classical exact equivalent. The quantum fluctuations present in the initial state of the environment must play a role in the "activation." One should note that these fluctuations are not "vacuum fluctuations" of the full system. Nevertheless, the fact that they have such a clear effect on the evolution of the system is quite remarkable. Whereas in the high-T case the quantum and classical oscillators composing the bath had identical distributions, they behave in a markedly different way as $T\to 0$. The quantum nature of the environment, which could be ignored at high T, leads in this limit to important non-negligible effects.

In terms of the master equation, the quantum fluctuations of the bath oscillators generate nonzero $f(t)$ and $D(t)$ terms, making diffusive phenomena possible. This is particularly true of the anomalous diffusion coefficient $f(t)$, which depends logarithmically on the cutoff Λ and thus can be considerably large [10]. Diffusion effects induced by quantum fluctuations are thus responsible for exciting the particle over the potential barrier. Though this process is very different from high-T thermal activation, we conjecture that it may still be interpreted in terms of a modified classical setting. The key ingredient is that the classical bath should mimic the properties of the quantum $T=0$ environment. Considering the classical and quantum versions of the noise kernel $\nu(s)$, it is possible to show that a bath of classical oscillators with a frequency-dependent temperature $T(\omega)=\hbar\omega/2$ should reproduce the effects of the initial quantum state. In fact, for this choice of classical environment one obtains $f(t)$ and $D(t)$ terms identical to those of the $T=0$ quantum case. Our main point is that after decoherence takes place, a quantum open system at $T=0$ should behave as a classical open system in contact with a classical bath whose oscillators are excited in a way that reproduces the fluctuations of the corresponding quantum environment. In order to fully understand this correspondence, one should simulate a classical system interacting with this type of generalized bath, reproducing the results of the quantum case and obtaining the same time scales for fluctuation-induced activation [12,22]. We will leave a detailed study of this type of system to a future publication [23].

A second question concerns the interplay of decoherence and excitation processes in the $T=0$ case. For both quantities, the value of the environment frequency cutoff Λ seems to play an important role, affecting both the decoherence time and the excitation process in the same direction. Since we do not have explicit estimates of the "activation" time in terms of Λ, it is hard to predict whether there is a regime for which decoherence happens fast enough and excitation is considerably delayed. Numerical results presented in Figs. 9 and 10 suggest that this is not possible. The two figures show, respectively, the probability to stay on the original well and the energy of the main system for several choices of the cutoff. Λ varies from the smallest frequency present in the system—i.e., the difference between the first-excited- and ground-state energy levels, E_1-E_0, and $\Lambda=10V_0$. Also shown are two intermediate cutoff values $\Lambda=V_0/10$ and $\Lambda=V_0$. By lowering Λ, the "activation" time is indeed postponed, but so is decoherence. In this situation the particle is simply able to tunnel back and forth between the two minima for a longer period. Higher values of the cutoff, on the other hand, lead to both fast decoherence and fast "activation." As a result we were never able to localize the particle in one of the wells, with tunneling and "activation" being simultaneously suppressed.

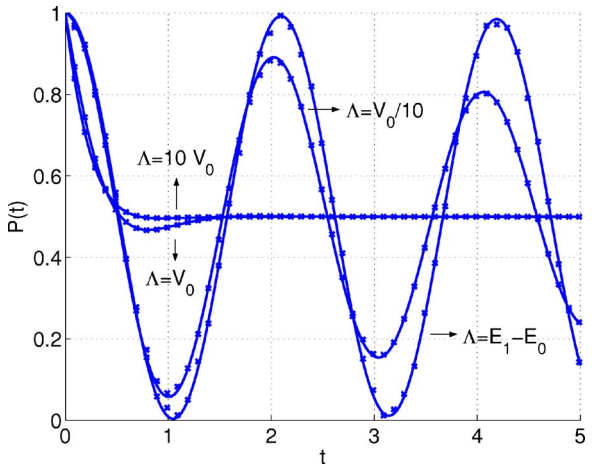

FIG. 9. (Color online) Probability to stay in the original well for different values of Λ (other parameters are fixed as in previous plots). The crosses are a subset of the simulation data (not all data points are shown so that the fit curves can be visible). The solid lines correspond to nonlinear χ^2 fits of the data to the expression in Eq. (35). Time is measured in units of the closed-system tunneling time τ.

The dependence of the activation time on the environmental cutoff frequency can be made more quantitative by fitting the probability for the particle to remain in the original well to a simple evolution expression. In Fig. 9 a selection of simulation points (crosses) is shown against a fit (solid curves) of the form

$$P(t)=\frac{1}{2}+\frac{1}{2}\cos(\pi t/\tau)\exp(-t/t_{\mathrm{act}}). \tag{35}$$

The analytical expression fits the data extremely well, allowing us to determine for each choice of Λ the two relevant

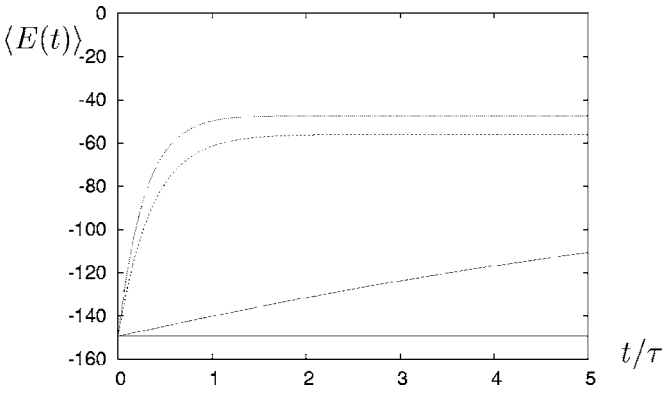

FIG. 10. Evolution in time of the mean energy of the main system for the same set of parameters as in Fig. 9 (time in units of the tunneling time τ). The solid lines correspond to the smallest value of Λ, the straight dashed line to $\Lambda=V_0/10$. Dotted lines are larger values of the cutoff: $\Lambda=10V_0$ on top and $\Lambda=V_0$ below.

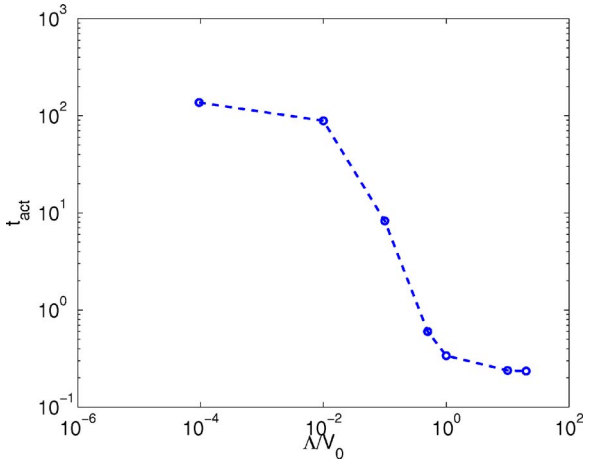

FIG. 11. (Color online) Log-log plot of the activation time t_{act} as a function of Λ/V_0.

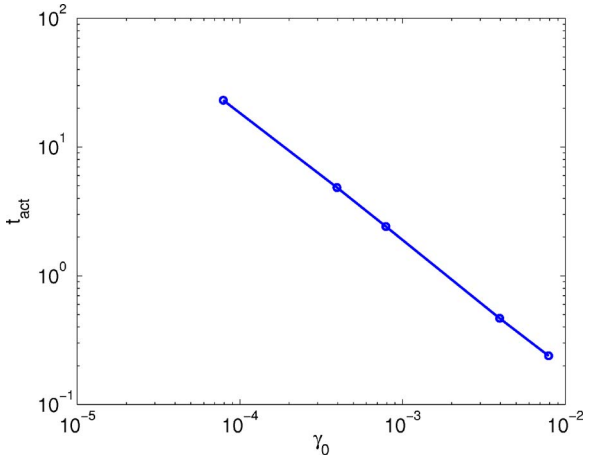

FIG. 12. (Color online) Log-log plot of the activation time t_{act} as a function of γ_0 for $\Lambda=10V_0$.

time scales τ and t_{act}. In Fig. 11 the activation time measured in this way is shown as a function of the cutoff parameter. This figure includes results for a larger number or curves, spanning several orders of magnitude of Λ. As expected the activation time decreases initially as the value of the cutoff increases. A change of regime is reached when Λ is of the order of magnitude of the height of the potential barrier V_0. For all values of $\Lambda < V_0$, tunneling is still observed, and indeed, the tunneling time, as measured by τ obtained from the fit, deviates very little—less than 5%—from the value for the isolated system. For higher values of Λ tunneling is completely suppressed, with the oscillating term in Eq. (35) becoming irrelevant for the fit. This suggests that $\Lambda \simeq V_0$ can be taken as the threshold for the fluctuations to play the principal role in the evolution, with excitation becoming the dominant processes in the dynamics in this regime. In all cases, the long-time-limit value for the probability seems to be 0.5 to a very good accuracy. As an extra check we refitted the data, allowing the asymptotic value of $P(t)$ as an extra free parameter. In the whole range of Λ studied, the final probability always differed by less than 0.8% from 0.5. The values for t_{act} obtained in the fit with the extra parameter changed by less than 6% when compared with the results shown in Fig. 11.

Similar properties can be observed in terms of the energy of the system in Fig. 10, where we plot the mean energy of the (main) system as a function of time, for the same set of parameters used in Fig. 9. Clearly, the "activation" process for high-frequency cutoff is accompanied by a fast increase in the energy of the system. Once again, the fact that the energy of the main system is considerably lower than the barrier height for low Λ supports the interpretation that quantum fluctuations are behind the excitation mechanism.

Finally, we looked at how the value of γ_0 affects the overall pattern of evolution, in the case of a cutoff $\Lambda=10V_0$. We found that as γ_0 decreases, as expected, tunneling reappears and the activation time increases as shown in Fig. 12. Interestingly the value of the measured tunneling time τ varies with γ_0. For very small values of the coupling, we obtain $\tau \sim 1$ in units of tunneling time. This value increases with γ_0 up to 50% of the original tunneling time. At this point, tunneling is suppressed and, as in the case discussed above, the oscillatory term in the fit can be ignored. This suggests that renormalization effects are likely to play a role in this case, as the strength of the interaction with the environment becomes larger. Also worth remarking is the fact that within the region of parameters tested, t_{act} seems to vary as the inverse of γ_0. This is reminiscent of Eqs. (32) and (34), indicating once again that decoherence and activation for this type of system are closely related. Overall, a very rich structure seems to emerge from the interplay of several physical mechanisms taking place simultaneously at $T=0$. A detailed numerical study of these will be the focus of a future publication.

V. FINAL REMARKS

We have analyzed a simple time-independent bistable system by following the quantum evolution of a particle initially localized at one of the minima of the potential when coupled to an external environment at both zero and high temperatures. When isolated, the particle undergoes tunneling through the barrier. For the open system, we described the effects of dissipation and diffusion on its dynamics in terms of three main phenomena: decoherence, tunneling, and thermal activation. We estimated the corresponding time scales analytically and showed that, depending on the parameters of the system and its environment, these processes can be made to act independently of the evolution. The numerical results confirmed the analytical estimates and allowed us to illustrate the distinct properties of the three types of process involved in the evolution.

For the closed system, the numerical simulations displayed all the expected features of standard quantum tunneling, with the wave packet bouncing back and forth between the two vacua, with a rate given by the estimated tunneling time τ. In the high-T regime, for an appropriate region of parameter space, the open system was shown to evolve in a fundamentally different way, with the probability for the particle to be found in the original well decaying at a much slower rate. With the basis of the relevant time scales deter-

mined analytically, we explained the absence of tunneling in this case as a consequence of early-time classicalization at t_D. The later-time evolution, on the other hand, was interpreted as a result of classical thermal activation. This picture was confirmed by looking at the evolution in terms of the space-probability distribution and the Wigner function. In contrast with the tunneling dynamics, the Wigner function for the open system became strictly positive soon after the decoherence time, evolving classically for most of the simulation time. For late times, the properties of the Wigner function were characteristic of thermal activation, with the phase-space separatrix becoming heavily populated as the particle crossed over the potential barrier. As an extra check, we evolved a similar classical system and confirmed that the concentration of probability around the separatrix at t_{th} does signal the onset of thermal activation. It is worth mentioning that the environment can, for both high and zero temperatures, be tailored so as to have tunneling before decoherence or in fact any other permutation of the three processes describing the dynamics. This can be easily seen by comparing the estimated time scales for each process. Though not shown here, we have checked numerically that all these cases are indeed possible.

The evolution of the open system at zero temperature shows subtly different and, in some ways, unexpected properties. Tunneling is also undoubtedly quickly suppressed, as can be seen by inspecting either the probability of the particle to remain on the original well or the evolution of its Wigner function. In both cases we observe typical classical features since very early times. Nevertheless, at $T=0$, the quantum fluctuations of the environmental oscillators, absent in a purely classical evolution, lead to nonzero diffusive terms. Their effect is felt primarily through the anomalous diffusion coefficient $f(t)$ that can have a large magnitude. We conjecture that these nontrivial diffusion effects induced by the quantum environment are large enough to excite the particle over the potential barrier. This is to be contrasted with the case where the environment is classical, forbidding any kind of activation phenomena. Though the late-time evolution in the presence of a quantum vacuum is by nature very different from high-T thermal activation, we suggest that it could still be interpreted in terms of a purely classical setting if the environment oscillators are described by a particular nonthermal statistical state. We will pursue this line of inquiry in depth in a forthcoming publication.

ACKNOWLEDGMENTS

We would like to thank E. Calzetta and J.P. Paz for comments and useful discussions. The work of N.D.A. was supported by PPARC. F.C.L. and P.I.V. were supported by CONICET, UBA, ANPCyT, and Fundación Antorchas. D.M. is supported by Fundación Antorchas and CIC.

APPENDIX

Written on the basis of the eigenstates $|\mu\rangle$ of the isolated system $H_{\mathrm{sys}}=\frac{p^2}{2}+V(x)$, Eq. (2) reads

$$\dot{\rho}_{\mu\nu}=-\imath\Delta_{\mu\nu}\rho_{\mu\nu}-\sum_{\alpha\beta\gamma}\rho_{\alpha\beta}\left[\int_0^t d\tau\nu(\tau)A^{\mu\nu}_{\alpha\beta\gamma}(\tau)-i\int_0^t d\tau\eta(\tau)B^{\mu\nu}_{\alpha\beta\gamma}(\tau)\right].$$

The time-dependent coefficients A and B are sums of four terms of the form $x_{\mu\alpha}x_{\alpha\beta}e^{\imath\Delta_{\gamma\alpha}\tau}$

$$\left.\begin{matrix}A^{\mu\nu}_{\alpha\beta\gamma}(\tau)\\ B^{\mu\nu}_{\alpha\beta\gamma}(\tau)\end{matrix}\right\}=x_{\mu\gamma}x_{\gamma\alpha}\delta_{\beta\nu}e^{-\imath\Delta_{\gamma\alpha}}\mp x_{\mu\alpha}x_{\beta\nu}e^{-\imath\Delta_{\beta\nu}}-x_{\mu\alpha}x_{\beta\nu}e^{-\imath\Delta_{\mu\alpha}}\pm x_{\beta\gamma}x_{\gamma\nu}\delta_{\alpha\mu}e^{-\imath\Delta_{\beta\gamma}}.$$

Thus, all the time integrals appearing in the master equation have the form

$$\int_0^t d\tau\nu(\tau)e^{\imath\Delta_{\alpha,\beta}\tau}\ \text{or}\ \int_0^t d\tau\eta(\tau)e^{\imath\Delta_{\alpha,\beta}\tau}.$$

These integrals can be explicitly calculated only if the spectral density of the environment is specified. We have supposed an Ohmic environment, for which $I(\omega)=2\gamma_0\frac{\omega}{\pi}\frac{\Lambda^2}{\Lambda^2+\omega^2}$, where Λ represents a high-frequency cutoff and γ_0 is a constant characterizing the strength of the interaction with the environment (we have set the mass equal to 1). For this environment the temperature-independent η integrals can be easily calculated to be

$$\int_0^t d\tau\eta(\tau)e^{\imath\Delta\tau}=\tilde{\Omega}^2(\Delta,t)+\imath\Delta\gamma(\Delta,t),$$

where

$$\tilde{\Omega}^2(\Delta,t)=-\frac{2\gamma_0\Lambda^3}{\Lambda^2+\Delta^2}\left[1-e^{-\Lambda t}\left(\cos\Delta t-\frac{\Delta}{\Lambda}\sin\Delta t\right)\right],$$

$$\gamma(\Delta,t)=\frac{\gamma_0\Lambda^2}{\Lambda^2+\Delta^2}\left[1-e^{-\Lambda t}\left(\cos\Delta t+\frac{\Lambda}{\Delta}\sin\Delta t\right)\right]$$

are the frequency-shift and dissipation coefficients, respectively.

The ν integrals are not so easily calculated, and so here we resort to a Markovian approximation. We will assume $\Lambda\gg\Delta_{\alpha\beta}\forall\,\alpha,\beta$. Thus, the kernels are strongly peaked around $t=\tau$ and the environment has a very short correlation time. Therefore the integrals can be extended over the entire interval $[0,\infty)$. If we further assume that the temperature is very high—that is, $T\gg\Delta_{\alpha\beta}\forall\,\alpha,\beta$—the ν kernel is reduced to a δ distribution function and the time integrals are simply[1]

$$\frac{\pi}{2}I(\Delta)\coth\left(\frac{\beta\Delta}{2}\right)\approx 2\gamma_0 T=D.$$

Finally, after some algebraic manipulations, the master equation reads as Eq. (19):

[1]Actually this last assumption accounts for the former one, for the high-temperature limit reduces to a Markovian approximation.

$$\dot{\rho}_{\mu\nu} = -\sum_{\alpha\beta} M_{\mu\nu\alpha\beta}\rho_{\alpha\beta},$$

where the *time-independent* coefficient M is

$$M_{\mu\nu\alpha\beta} = \imath\,\delta_{\alpha\mu}\delta_{\beta\nu}\Delta_{\alpha\beta} + L_{\mu\nu\alpha\beta} - \imath N_{\mu\nu\alpha\beta},$$

with

$$L_{\mu\nu\alpha\beta} = \sum_{\gamma}[x_{\mu\gamma}x_{\gamma\alpha}\delta_{\nu\beta}K^{+}_{\gamma\alpha} - x_{\mu\alpha}x_{\alpha\gamma}K^{-}_{\beta\nu} - x_{\mu\alpha}x_{\beta\nu}K^{+}_{\mu\alpha} + x_{\beta\gamma}x_{\gamma\nu}\delta_{\alpha\mu}K^{-}_{\beta\gamma}],$$

$$N_{\mu\nu\alpha\beta} = \sum_{\gamma}[x_{\mu\gamma}x_{\gamma\alpha}\delta_{\nu\beta}S_{\gamma\alpha} - x_{\mu\alpha}x_{\alpha\gamma}S_{\beta\nu} - x_{\mu\alpha}x_{\beta\nu}S_{\mu\alpha} + x_{\beta\gamma}x_{\gamma\nu}\delta_{\alpha\mu}S_{\beta\gamma}],$$

$$K^{\pm}_{\alpha\beta} = K^{\pm}(\Delta_{\alpha\beta}), \quad S_{\alpha\beta} = S(\Delta_{\alpha\beta}),$$

$$K^{\pm}(\Delta) = \frac{\pi}{2}I(\Delta)\coth\left(\frac{\beta\Delta}{2}\right) \pm \Delta Y(\Delta),$$

$$S(\Delta) = \Lambda Y(\Delta),$$

$$Y(\Delta) = \gamma_0\frac{\Lambda^2}{\Lambda^2 + \Delta^2}.$$

[1] C. Monroe *et al.*, Science **272**, 1131 (1996); C. J. Myatt *et al.*, Nature (London) **403**, 269 (2000); M. Brune, E. Hagley, J. Dreyer, X. Maitre, A. Maali, C. Wunlerlich, J. M. Raimond, and S. Haroche, Phys. Rev. Lett. **77**, 4887 (1996); A. Rauschenbeutel *et al.*, Science **288**, 2024 (2000); J. R. Friedman *et al.*, Nature (London) **406**, 43 (2000); C. H. van del Wal *et al.*, Science **290**, 773 (2000); C. Tesche, *ibid.* **290**, 720 (2000).

[2] J. P. Paz and W. H. Zurek, in *Coherent Matter Waves*, Les Houches Session LXXII, edited by R. Kaiser, C. Westbrook, and F. David, EDP Sciences (Springer-Verlag, Berlin, 2001) pp. 533–614; W. H. Zurek, Rev. Mod. Phys. **75**, 715 (2003).

[3] A. O. Caldeira and A. J. Leggett, Phys. Rev. Lett. **46**, 211 (1981); Ann. Phys. (N.Y.) **149**, 374 (1983).

[4] U. Weiss, *Quantum Dissipative Systems* (World Scientific, Singapore, 1993); J. M. Martinis, M. H. Devoret, and J. Clarke, Phys. Rev. B **35**, 4682 (1987); A. Wallraff, T. Duty, A. Lukashenko, and A. V. Ustinov, Phys. Rev. Lett. **90**, 037003 (2003).

[5] P. Hänggi, P. Talkner, and M. Borkovek, Rev. Mod. Phys. **62**, 251 (1990).

[6] S. Coleman, *Aspects of Symmetry* (Cambridge University Press, New York, 1985).

[7] J. P. Paz, S. Habib, and W. H. Zurek, Phys. Rev. D **47**, 488 (1993).

[8] W. H. Zurek, in *The Physical Origin of Time Asymmetry*, edited by J. J. Halliwell, J. Perez Mercader, and W. H. Zurek (Cambridge University Press, Cambridge, UK, 1994).

[9] L. Dávila Romero and J. P. Paz, Phys. Rev. A **55**, 4070 (1997).

[10] F. C. Lombardo and P. I. Villar, Phys. Lett. A **336**, 16 (2005).

[11] M. Buttiker, e-print cond-mat/0106149.

[12] E. Calzetta and E. Verdaguer, e-print quant-ph/0407185.

[13] B. L. Hu, J. P. Paz, and Y. Zhang, Phys. Rev. D **45**, 2843 (1992) ; **47**, 1576 (1993).

[14] A. J. Leggett, S. Chakravarty, A. T. Dorsey, M. P. A. Fisher, A. Garg, and W. Zwerger, Rev. Mod. Phys. **59**, 1 (1987).

[15] J. Ankerhold and H. Grabert, Phys. Rev. Lett. **91**, 016803 (2003); E. Calzetta, A. Roura, and E. Verdaguer, *ibid.* **88**, 010403 (2002).

[16] W. A. Lin and L. E. Ballentine, Phys. Rev. A **45**, 3637 (1992); R. Uttermann, T. Dittrich, and P. Hänggi, Phys. Rev. E **49**, 273 (1994); T. Dittrich, B. Oelschlaegel, and P. Hänggi, Europhys. Lett. **22**, 5 (1993); S. Kohler, R. Utermann, P. Hänggi, and T. Dittrich, Phys. Rev. E **58**, 7219 (1998).

[17] D. Monteoliva and J. P. Paz, Phys. Rev. Lett. **85**, 3373 (2000); Phys. Rev. E **64**, 056238 (2001).

[18] F. C. Lombardo, F. D. Mazzitelli, and D. Monteoliva, Phys. Rev. D **62**, 045016 (2000).

[19] S. Chaturvedy and F. Shibata, Z. Phys. B **35**, 297 (1979); D. F. Walls and G. J. Milburn, *Quantum Optics* (Springer-Verlag, Berlin, 1994).

[20] S. Takagi, *Macroscopic Quantum Tunneling* (Cambridge University Press, Cambridge, UK, 2002).

[21] N. D. Antunes, F. C. Lombardo, and D. Monteoliva, Phys. Rev. E **64**, 066118 (2001).

[22] D. Arteaga, E. Calzetta, A. Roura, and E. Verdaguer, Int. J. Theor. Phys. **42**, 1257 (2003).

[23] N. D. Antunes, F. C. Lombardo, D. Monteoliva and P. I. Villar, *in preparation*.